

Self-adaptive vision-language model for 3D segmentation of pulmonary artery and vein

Xiaotong Guo^{*2}, Deqian Yang^{*1,3}, Dan Wang³, Haochen Zhao⁵, Yuan Li⁸,
Zhilin Sui², Tao Zhou⁴, Lijun Zhang^{†1}, and Yanda Meng^{†6,7}

¹Key Laboratory of System Software (Chinese Academy of Sciences) and
State Key Laboratory of Computer Science, Institute of Software, Chinese Academy of Sciences, China.

²Department of Thoracic Surgery, National Clinical Research Center for Cancer/Cancer Hospital Shenzhen Hospital

³School of Intelligent Science and Technology, Hangzhou Institute for Advanced Study,
University of Chinese Academy of Sciences, Hangzhou 310024, China.

⁴R&D Center, Guangxi Huayi Artificial Intelligence Medical Technology Co., Ltd

⁵School of Computer Science and Engineering, Beihang University, Beijing, China.

⁶Department of Computer Science, University of Exeter, Exeter, UK.

⁷Department of Cardiovascular & Metabolic Medicine, University of Liverpool, Liverpool, UK.

⁸Guangzhou Jiayi Software Technology Co., Ltd.

[†]Corresponding author: zhanglj@ios.ac.cn , Y.m.meng@exeter.ac.uk

Abstract—Accurate segmentation of pulmonary structures is crucial in clinical diagnosis, disease study, and treatment planning. Significant progress has been made in deep learning-based segmentation techniques, but most require much labeled data for training. Consequently, developing precise segmentation methods that demand fewer labeled datasets is paramount in medical image analysis. The emergence of pre-trained vision-language foundation models, such as CLIP, recently opened the door for universal computer vision tasks. Exploiting the generalization ability of these pre-trained foundation models on downstream tasks, such as segmentation, leads to unexpected performance with a relatively small amount of labeled data. However, exploring these models for pulmonary artery-vein segmentation is still limited. This paper proposes a novel framework called Language-guided self-adaptive Cross-Attention Fusion Framework. Our method adopts pre-trained CLIP as a strong feature extractor for generating the segmentation of 3D CT scans, while adaptively aggregating the cross-modality of text and image representations. We propose a specially designed adapter module to fine-tune pre-trained CLIP with a self-adaptive learning strategy to effectively fuse the two modalities of embeddings. We extensively validate our method on a local dataset, which is the largest pulmonary artery-vein CT dataset to date and consists of 718 labeled data in total. The experiments show that our method outperformed other state-of-the-art methods by a large margin. Our data and code will be made publicly available upon acceptance.

Index Terms—Vision Language Model, Pulmonary Artery and Vein Segmentation, CLIP

I. INTRODUCTION

In recent years, pulmonary vascular diseases, including pulmonary embolism and pulmonary hypertension, have emerged as one of the conditions with the highest morbidity and mortality rates. Computed tomography (CT) has been widely adopted as a diagnostic tool to elucidate tomographic patterns

of pulmonary diseases [1]. Therefore, implementing automated pulmonary vascular segmentation is of significant clinical importance for achieving a three-dimensional reconstruction of the pulmonary vascular architectures. However, the manual delineation process remains labour-intensive due to the complexity of tubular structures. Segmentation methods for lung vessels have primarily focused on Convolutional Neural Networks (CNNs), particularly the U-Net architecture and its variants. These approaches have effectively maximized the potential of limited labeled data, especially from CT scans. Many semi-supervised and weakly supervised learning approaches are proposed based on pseudo labeling of the partially labeled data [2]–[10]. However, they often suffer significantly from the incorrectness of pseudo labels associated with unlabeled parts of the CT data.

Recently, a new learning paradigm known as the Vision-Language Model (VLM) pre-training and zero-shot prediction has gained significant attention. This paradigm involves pre-training a vision-language model using large-scale image-text pairs abundantly available online. The pre-trained VLM can be directly applied to downstream visual recognition tasks without fine-tuning. For example, CLIP [11] employs an image-text contrastive objective by bringing paired images and texts closer together in the embedding space while pushing unpaired ones further apart. Numerous efforts are being made to adapt VLMs to specific task domains. For example, some approaches [11]–[13] modify the contrastive objectives to generative or alignment objectives to retrain a VLM. On the other hand, other methods fine-tune existing VLMs at a lower cost, including techniques such as prompt tuning [14] and feature adapters [15]. Regarding medical image segmentation, models such as SAM [16] and its variants [17],

* These authors have contributed equally to this work.

[18] have been retrained on medical images (e.g., Med-SAM [18], SAM-MED3D [17]), achieving significant success in this area. However, the required use of box or point prompts is unsuitable for artery-vein segmentation. This is because the ends of pulmonary vessels are quite intricate to locate in CT scans, as illustrated in Fig. 3. This complexity necessitates extensive box or point labeling to achieve satisfactory masks, rendering the process labour-intensive.

This work introduces an efficient language-guided self-adaptive cross-attention fusion framework that integrates adaptive modules designed explicitly for pulmonary artery/vein (A/V) segmentation tasks. Our model not only preserves the performance of the pre-trained model to a great extent but also leverages the unique characteristics of data collected in local hospital settings more effectively. By incorporating these adaptive modules, our framework achieved an average DSC score of 76.22% on A/V segmentation, significantly surpassing the performance of the current state-of-the-art methods, such as nnU-Net [19] by an average DSC score of 9.03%, and nnFormer [20] by an average DSC score of 12.37%. The primary contributions of this study are as follows:

(1) We exploit a large pre-trained vision-language model to segment pulmonary arteries and veins using a substantial local dataset comprising 718 annotated CT scans. The proposed dataset will be made publicly available upon acceptance.

(2) We propose an adaptive module incorporating attention mechanisms and data augmentation methods that are specially designed for our dataset to highlight the vascular characteristics of pulmonary arteries and veins. These mechanisms significantly enhance the fusion of features between the language and visual models, yielding awe-inspiring results on the test dataset.

(3) Extensive experiments on a large number of annotated CT data have been conducted to validate the effectiveness of our proposed methods. The results of these experiments have demonstrated significant performance improvement over other state-of-the-art methods.

II. RELATED WORK

A. Vision language models in medical imaging

Recently, VLMs have achieved significant advancements in cross-modal tasks and visual recognition problems, as exemplified by models such as CLIP [11] and ALIGN [21]. CLIP, a pioneering work in large-scale vision-language pre-training, utilized contrastive learning to learn image representations from a dataset of 400 million (image, text) pairs. Inspired by CLIP and ALIGN, a substantial number of medical image-text pairs have been employed to train VLMs through contrastive learning as foundation models. For instance, PMC-CLIP [22] was trained on over 1M medical image-text pairs, while BiomedCLIP [23] was trained on over 15M pairs. The majority of their research efforts have been directed towards medical visual question-answering tasks, aiming to provide pre-trained models that capture the similarity between text and medical images. There has been a scarcity of work focusing on the medical image segmentation domain. Notably, Liu et al.

[24], [25] utilized the original CLIP encoder embedding fused with a segmentation network encoder embedding to address the issue of partial labeling in abdominal organ segmentation, achieving the top rank in the Medical Segmentation Decathlon competition [26].

B. Pulmonary vascular segmentation

The segmentation of pulmonary arteries and veins remains an open challenge. In recent years, many studies have adopted 2D or 3D U-Net [27], [28] to automatically extract features, achieving satisfying performance. However, accurate vascular segmentation remains challenging due to the scarcity of high-quality open-sourced datasets: the extreme complexity of the vascular tree structure, the close proximity (often interwoven) of arteries and veins, and their similar intensity values (especially in non-contrast CT). The Parse2022 [29] competition provided 100 CT images for arterial segmentation, and the top-ranked participant used Res-U-Net [30] combined with threshold segmentation for arterial segmentation. Similarly, Qi et al. [31] proposed to extract semantic embedding in a dual U-Net architecture. This study is based on 57 CT datasets from LUNA16 [32], with initial artery and vein labels generated using region growing in the lung vessel mask. Differently, in this work, we propose the largest pulmonary artery-vein dataset to date, which comprises 718 CT scans that are finely annotated by clinicians.

III. METHODS

CLIP (Contrastive Language-Image Pre-training) is a pre-training method developed by OpenAI [11]. Built upon the methodology of contrastive pre-training [33], it jointly optimizes a vision encoder and a text encoder, where the vision encoder is based on either ResNet [34] or Vision Transformer (ViT) [35]. The language encoder is rooted in a transformer-based model like BERT [36], forcing the paired image-text information to be as close as possible to the joint image-text latent space after encoding. We adopt the original CLIP model as our text embedding extractor. Trained on a vast collection of image-text pairs, CLIP learns visual representation through text supervision, known as prompt. We design a specialized prompt for our pulmonary vessel segmentation task, as seen in Table. I.

A. Pretrained text encoder and vision model

Text encoder: We use the original pre-trained CLIP encoder E_{text} with a specially designed medical prompt (i.e. ‘A computerized tomography of a category with small branches’) to generate text embeddings $H_t \in \mathbb{R}^{K \times D}$, where K represents the number of class, and D represents the length of the embedding. The pre-trained encoder consists of a 12-layer 512-wide transformer with eight attention heads. The 512-wide output of the transformer is used as text embedding. To enhance the CLIP architecture’s medical capability for medical image segmentation tasks, we use K text adapters A_{text} to fine-tune E_{text} . We observe that the selection of medical prompt templates is hand-crafted and worthy of experiments.

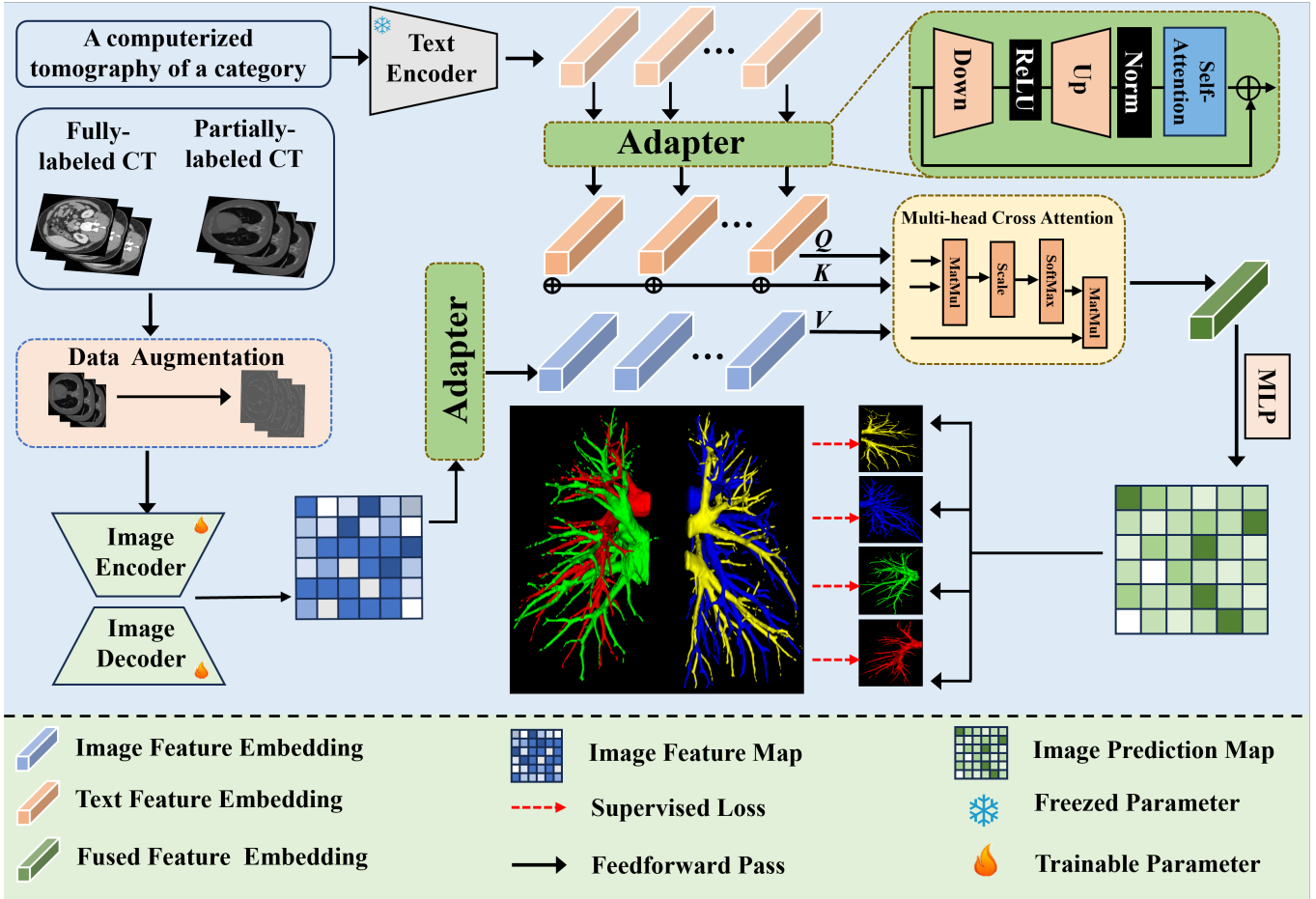


Fig. 1. Overview of the proposed Language-guided self-Adaptive Cross-Attention Fusion Framework, which comprises a text encoder and an image segmentation model. Our model can adaptively learn suitable embedding for the left/right vein and artery. Best viewed in color.

Table I illustrates the effectiveness of four different prompt templates. The last template, specifically designed for our vascular-shaped data, demonstrates nearly a 0.1% improvement compared to other commonly used templates, indicating that adjusting the prompt benefits our model.

TABLE I
ABLATION STUDYS OF DIFFERENT PROMPTS.

Embedding	prompt	DSC(%) \uparrow
train:val:test = 502:72:143(Fully labeled + Half-labeled)		
CLIP v1	A photo of a category	74.35 _{0.36}
CLIP v2	A computerized tomography of a category	75.74 _{0.24}
CLIP v3	There is a category in this computerized tomography	76.03 _{0.37}
CLIP v4	A computerized tomography of a category with small branches	76.22 _{0.48}

$$H_t = E_{text}(x_{text}), \quad (1)$$

$$H_t^a = A_{text}(H_t). \quad (2)$$

Vision model: Medical Segmentation Decathlon [26] is a benchmark for many medical organ segmentation tasks. Specifically, Liu et al. [24] ranked first with an open-source pre-trained model¹ U-Net and Swin UNETR. Accounting for its strong ability to segment organs, the pre-trained model minimizes the time cost of training a model and inherits the weights that are suitable for organ segmentation. Therefore, we adopt a pre-trained U-Net model as the backbone for segmentation. Specifically, in our model, the 3D CT images $x_{img} \in \mathbb{R}^{H*W*L}$ are encoded into a feature map $V \in \mathbb{R}^{B*C*H*W*L}$ through the U-Net encoder E_{img} , where B represents batch and C represents channels. An image adapter A_{img} is used to map every batch B of raw high-level features to the embedding $H_v^a \in \mathbb{R}^{B*D}$.

¹<https://github.com/ljwztc/CLIP-Driven-Universal-Model>

$$H_v = E_{img}(x_{img}), \quad (3)$$

$$H_v^a = A_{img}(H_v), \quad (4)$$

To match the shape of H_t , we duplicate H_v^a according to the class number K . We define:

$$\text{rep}(H, k) = \text{concat} \underbrace{[H, H, \dots, H]}_{k \text{ times}}, \quad (5)$$

then, we obtain the result $H_v^a \in \mathbb{R}^{B \times K \times D}$,

$$H_v^a = \text{rep}(A_{text}(H_v), K). \quad (6)$$

B. Attention-based self adaptive learning pipeline

The vision language models have shown promising results across various tasks, attributable to their generalizability and interpretability. However, they often face the image and text distribution gap when applied to downstream tasks. For example, a medical segmentation dataset may have task-specific image styles and text formats that are not included in the pre-trained data sources. Therefore, how to fine-tune the pre-trained model at a lower cost and how to fuse different modalities of embeddings can be a noteworthy problem. We propose an attention-based self-adaptive learning pipeline to address the problem effectively.

In detail, the capability of CLIP is rooted in the natural image-text pairs. We enhance it for medical image segmentation tasks through fine-tuning. During training, the pre-trained CLIP encoder maintained frozen instead of fully adjusting all parameters to reduce the computing workload. We devise an adapter module and integrate it into designated positions shown in Fig 1. The adapter consists of a down-projection, ReLU activation, and up-projection with batch normalization and self-attention sequentially. The down-projection compresses the given embedding into a lower dimension using an MLP layer. At the same time, the up-projection expands the compressed embedding back to its original dimension using another MLP layer. Self-attention calculation captures the correlation of each class. The adapter trains CLIP embedding at a low cost with frozen parameters while intensely learning the attention of each class, guiding the segmentation model through the fusion method. Additionally, a trainable adapter is introduced into the vision model component, which is based on a pre-trained U-Net due to its manageable parameter size, making it an efficient starting point for training. This adapter facilitates the transition from image features to embeddings, enhancing the segmentation process.

In terms of fusing text and image embeddings after adopting the vision language model as the backbone, Lin et al. [37], Zhou et al. [38] and Liu et al. [24] adopt simple strategies, such as direct plus or concatenation. Differently, we adopt the cross-attention(CA) module to integrate the two domain embeddings adaptively. The attention function serves as the operation to discover inner relationships from one modality to another. We

have used the aforementioned adapters to get text embedding $H_t^a \in \mathbb{R}^{B \times K \times D}$ and image embedding $H_v^a \in \mathbb{R}^{K \times D}$, for every batch $H_t^a(b)$, we calculate the attention scores H_f :

$$f_{CA}(H) = \text{softmax} \left(\frac{q(H_t^a)^T k(H_t^a + H_v^a(b))}{\sqrt{d_k}} \right) v(H_v^a(b)). \quad (7)$$

The input sequences of these two modalities are identically ordered in our input. Based on this, contextual clues can be propagated between modalities. As for the cross-attention module's detail, we choose the text embedding to be query (Q), image embedding to be value (V), and the plus of them to be the key (K). With language embedding's guidance, more precise features can be automatically selected rather than concatenated or plus in a hand-crafted way. The alignment of image and text embedding H_f uses a multi-layer perceptron (MLP) to generate parameters (θ_k) . Three sequential convolutional layers with $1 \times 1 \times 1$ kernels filling with (θ_k) convert vision decoder output features F into k predictions, where $P_k = \text{Sigmoid}((F * \theta_{k_1}) * \theta_{k_2}) * \theta_{k_3}$, $\theta_k = \{\theta_{k_1}, \theta_{k_2}, \theta_{k_3}\}$. $*$ represents convolution operation. For each class k , we get every foreground class $P_k \in \mathbb{R}^{1 \times H \times W \times L}$. After that, we merge k classes of prediction into one prediction P , shown in Fig 1. P_k is supervised by label Y_k , where the overall loss is represented as:

$$\mathcal{L}_{sup} = \frac{1}{|B|} \sum_{i=1}^{|B|} [\mathcal{L}_S(P_k, Y_k)], \quad (8)$$

where $\mathcal{L}_S = \frac{1}{2} [\mathcal{L}_{Dice} + \mathcal{L}_{ce}]$; \mathcal{L}_{Dice} and \mathcal{L}_{ce} represent the Dice and cross-entropy losses, respectively. The pseudo code of our framework can be found on Alg. 1

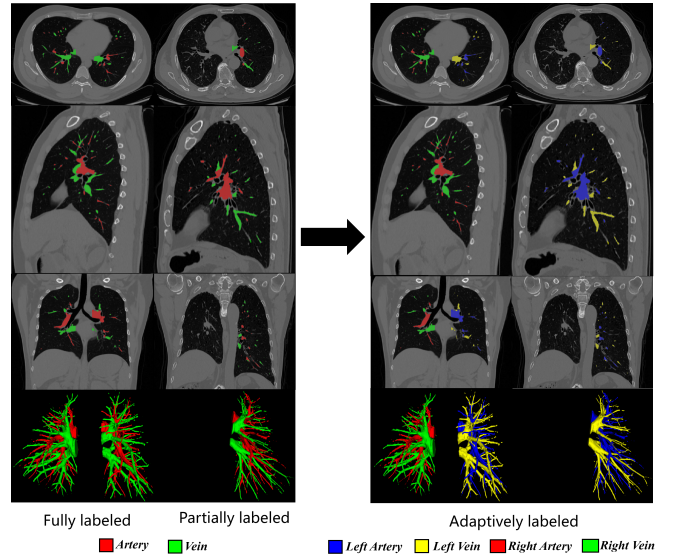


Fig. 2. This pic shows the adaptation of our data. We only change the label of the artery/vein without making any other adjustments.

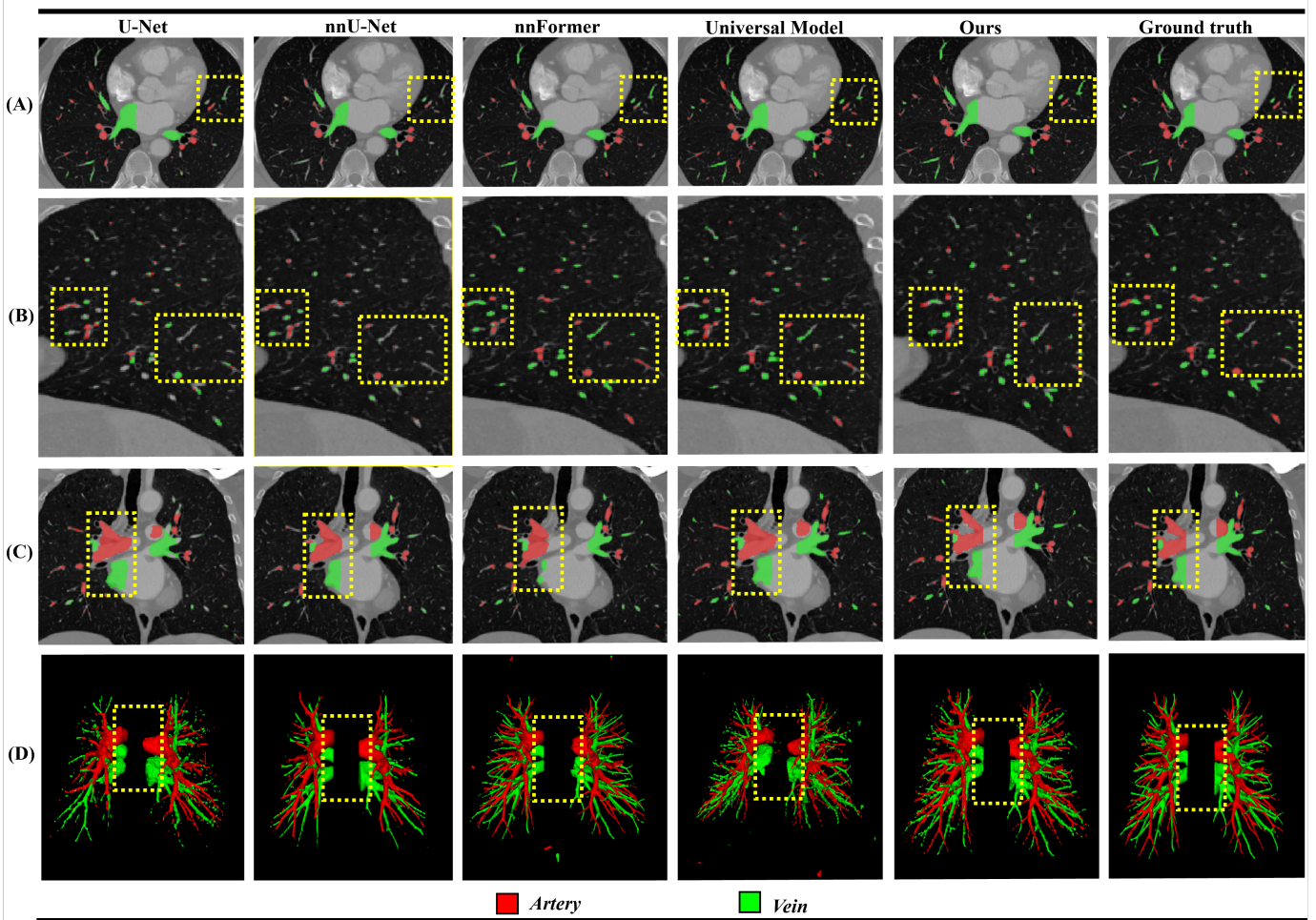


Fig. 3. Visualization of segmentation results on our dataset with zoomed-in views for enhanced clarity. (A-D) The segmentation results of one case are presented in the transverse section, coronal section, sagittal section, and 3D view, respectively. The regions enclosed by the dashed yellow boxes indicate misclassification executed by other models; our method can segment those regions closer to the ground truth. Mask colors for vessels have been standardized to red for arteries and green for veins to better visualize the differences between the methods.

IV. DATASET AND IMPLEMENTATION DETAIL

A. Dataset:

We present a large-scale pulmonary vessel segmentation dataset collected from a real-world local hospital, comprising a total of 718 3D CT volumes provided in compressed NIFTI (.nii.gz) format. Among these, the pulmonary arteries and veins are manually annotated, where 79 CT scans are fully labeled and 639 CT scans are half-labeled, indicating the involvement of either the left lung or the right lung, as depicted in Fig. 2. In clinical practice, most patients typically exhibit disease in only one lung, with only a small proportion affected in both lungs. Therefore, it is reasonable to compile a dataset that combines fully labeled and half-labeled CT scans. The sizes of these CT volumes range from $512 \times 512 \times 169$ to $512 \times 512 \times 985$, with varying slice thicknesses from 0.62 to 1.25 mm. Annotations are obtained from five junior clinicians (with one to five years of experience) who used MIMICS to manually refine the segmentation results under the supervision

of two board-certified radiologists. Finally, a senior radiologist with over ten years of experience verified and refined the annotations. We will make the dataset and annotations publicly available upon the acceptance of this work. We divide the labeled data into training, validation, and test sets at a ratio of 7:1:2, where 502 volumes are designated as the Training Dataset; 72 volumes are allocated for validation and 143 volumes for testing. Results are shown on Tabel IV. All experiments are reported as $mean_{std}$ with three repeated trials in this work.

B. Implementation detail:

Our model is implemented with U-Net as the backbone and optimizing the parameters via AdamW [39]. The training utilizes a batch size of 4 and a patch size of $96 \times 96 \times 96$. The default initial learning rate is set to $8e-4$, with a momentum of 0.9 and a decay of $1e-5$. The framework is implemented in MONAI version 0.9.05. The best model is selected within 200 epochs by evaluating the validation metrics. Models are

Algorithm 1: Training Procedure of Our Method

Data:
Half-labeled data $D^p = \{(x_i, y_i)\}_{i=1}^N (y_i = 1, 2)$,
Fully labeled data $D^f = \{(x_i, y_i)\}_{i=1}^M (y_i = 1, 2)$

Input:
Processed labeled data $D^m = \{(x_i, y_i)\}_{i=1}^{N+M} (y_i = 1 : 4)$,
Segment network encoder S_{enc} , Segment network decoder S_{dec} ,
CLIP encoder T_{enc} , batchsize \mathcal{B} , number of classes num_class ,
max epoch E_{max}

Output:
Trained weights of model $f(\cdot; \theta)$

```

1 for epoch in  $E_{max}$  do
2   for batch in  $\mathcal{B}$  do
3     Freeze CLIP model  $T_{enc}$ 
4     Initialize  $num\_class$  Adapter  $Adp_{text}$ 
5     Initialize one Adapter  $Adp_{img}$ 
6     Get text embedding feature  $H_t \leftarrow T_{enc}$ 
7     Get segment embedding feature  $H_v \leftarrow S_{enc}(x_i)$ 
8     Calculate  $H_t^a \leftarrow Adp_{text}(t)$ 
9     Calculate  $H_v^a(batch) \leftarrow Adp_{img}(H_v^a(batch))$ 
10     $H_v^a \leftarrow rep(H_v^a, num\_class)$  according to Eqs. (5)
11     $H_f \leftarrow Cross\_attention(H_t^a, H_v^a + H_t^a, H_v^a)$  // get
        mixed feature map
12    Calculate  $\mathcal{L}_{sup}$  according to Eqs. (8)
13    Update  $\mathcal{L}_{sup}$  according to Eqs. (8)
14  end
15  epoch = epoch + 1
16 end
17 return model  $f(\cdot; \theta)$ 

```

TABLE II

NNU-NET PREPROCESS EXPERIMENTS UNDER DIFFERENT DATASET SETTING.

Methods	DSC(%) \uparrow	Jaccard(%) \uparrow
train:val:test = 64:6:7(Fully labeled)		
nnU-Net	66.14 \pm 0.27	54.31 \pm 0.15
Ours	69.34 \pm 0.24	58.32 \pm 0.11
train:val:test = 502:72:143(Fully labeled + Half-labeled)		
nnU-Net	67.19 \pm 0.12	56.45 \pm 0.34
Ours	76.22 \pm 0.76	62.74 \pm 0.45

trained on a single 40 GB NVIDIA A100 card. The Dice Similarity Coefficient (DSC), Normalized Surface Distance (NSD), Jaccard and 95% Hausdorff distance (HD95) are used to evaluate vessel segmentation performance in this work.

Data augmentation: As mentioned above, our data consists of both fully and half-labeled datasets with annotations: for example, we use 1 to represent the annotations of the pulmonary artery and 2 for the pulmonary vein. However, due to the complexity of tubular structures and the close intensity values of pulmonary vessels and airways in CT scans, segmenting the pulmonary vessels is quite challenging. Therefore, we adopt strong augmentation techniques for both CT input and label ground truth.

CT augmentation: Firstly, we adjusted the window width and level to meet the appropriate Hounsfield unit for pulmonary vessels, ranging from -700 to 300. Then, we calculate the Hessian matrix of the CT and obtain the eigenvalue to fill the Z-axis, which strengthens the CT’s tubular structures, as shown in Fig 1.

Label augmentation: We convert the three-class segmentation task (*i.e.* background, artery, vein) into a five-class segmentation task. For example, we represent 1 for the left pulmonary artery, 2 for the left pulmonary vein, 3 for the right pulmonary artery, 4 for the right pulmonary vein and 0 for the background. This method can improve the model’s performance significantly, not only for us but other state-of-the-art methods as well. It can be seen from Table II that when adding the half-labeled data into training without adaptive augmentation, the DSC slightly increased from 66.14% to 67.19%. This means that the incomplete label is not exploited in this setting. Instead, our method utilizes these settings and gets the full potential of the half-labeled data. Therefore, we choose a simple but efficient augmentation for our incomplete label.

TABLE III

ABLATION STUDY OF EVERY COMPONENT OF OUR FRAMEWORK. UM INDICATES UNIVER MODEL, DA INDICATES DATA AUGMENTATION, AAP INDICATES ATTENTION-BASED SELF ADAPTIVE LEARNING PIPELINE

UM	DA	AAP	DSC(%) \uparrow	Jaccard(%) \uparrow	NSD \downarrow	HD95 \downarrow
\checkmark			64.49 _{0.45}	56.32 _{0.15}	0.98 _{0.03}	47.34 _{0.35}
\checkmark	\checkmark		68.38 _{0.25}	58.33 _{0.02}	0.91 _{0.06}	46.43 _{0.01}
\checkmark	\checkmark	\checkmark	76.22 _{0.76}	62.74 _{0.24}	0.86 _{0.43}	14.48 _{0.22}

V. EXPERIMENTS

A. Ablation studies

We conduct ablation studies to evaluate every component of our proposed pipeline. The quantitative results of the different methods are presented in Table. III with DSC, Jaccard, NSD and HD95. The pre-trained Univer Model(UM) [24] is used as our baseline. We first use a simple Data Augmentation(DM) to effectively use our half-labeled data, contributing a performance gain of over 3.89% DSC, 2.01% Jaccard over baseline, reduces 0.007 NSD and 0.91 HD95 compared with baseline. Subsequently, our proposed attention-based self-adaptive learning pipeline is introduced to fine-tune the pre-trained model and align text representations with image representations with an adaptive attention mechanism. We observe a further increment of 7.84% in DSC, 4.41% in Jaccard and a significant decrement of 31.95 in HD95, 0.05 in NSD.

B. Comparison of quantitative results on test dataset

Table IV presents a qualitative comparison of our proposed vessel test dataset, which consists of 143 CT volumes, against other state-of-the-art methods. As shown in Table II, nnU-Net [19] demonstrated promising results, achieving a mean DSC of 66.14% and a mean Jaccard of 54.31% when trained on a fully labeled dataset. However, when a substantial amount of half-labeled data is incorporated into the training process, nnU-Net only improved by 1.05% in DSC. In contrast, our framework achieved a DSC of 69.34% and a Jaccard of 58.32% with a small fully labeled dataset, and demonstrated a significant increase of 6.88% in DSC when utilizing all available labeled data. We speculate that the notable decrease

TABLE IV

SUMMARY OF EXPERIMENTAL RESULTS ON THE PROPOSED DATASET, DETAILING THE COMPARISON OF OUR METHODS WITH EXISTING APPROACHES FOR THE CLASSES OF ARTERY AND VEIN. THE REPORTED METRICS INCLUDE DSC, JACCARD, NSD, AND HD95. METRICS ARE PRESENTED IN THE FORM OF $mean \pm std$, WHERE EACH METHOD IS EVALUATED OVER THREE TRIALS FOR AVERAGING.

Methods	Artery				Vein				Mean DSC
	DSC(%) \uparrow	Jaccard(%) \uparrow	NSD \downarrow	HD95 \downarrow	DSC(%) \uparrow	Jaccard(%) \uparrow	NSD \downarrow	HD95 \downarrow	
U-Net [40]	61.23 _{0.48}	48.34 _{0.38}	1.94 _{0.19}	132.23 _{1.32}	59.38 _{0.49}	49.32 _{0.49}	1.43 _{0.14}	110.76 _{1.11}	60.49 _{0.60}
nnU-Net [19]	67.52 _{0.63}	56.45 _{0.56}	0.81 _{0.05}	43.76 _{0.51}	66.86 _{0.56}	55.81 _{0.21}	0.77 _{0.08}	44.35 _{0.44}	67.19 _{0.67}
nnFormer [20]	64.46 _{0.51}	51.32 _{0.12}	0.89 _{0.06}	86.61 _{0.87}	63.25 _{0.82}	52.67 _{0.53}	0.85 _{0.09}	96.32 _{0.96}	63.85 _{0.64}
Universal Model [24]	70.24 _{0.57}	57.25 _{0.57}	0.79 _{0.02}	25.34 _{1.78}	69.32 _{0.54}	54.32 _{0.55}	0.77 _{0.06}	28.97 _{1.16}	69.78 _{0.69}
Ours	77.26 _{0.64}	64.13 _{0.61}	0.86 _{0.05}	13.72 _{0.14}	75.19 _{0.23}	61.34 _{0.15}	0.86 _{0.09}	15.24 _{0.15}	76.22 _{0.76}

in performance of nnU-Net compared to our framework is attributable to the ambiguity introduced by the additional half-labeled data. For instance, fully labeled CT scans annotate both left and right arteries, whereas half-labeled scans may only specify left or right arteries, leaving the other unlabeled. Thus, merely adding more data does not necessarily enhance model training. Therefore, we report the performance metrics of other state-of-the-art methods trained on the fully labeled dataset but tested on the 143 CT volumes. The universal model achieved a mean DSC of 69.78%, as shown in Table IV, which is 5.29% higher than the universal model trained on all dataset settings, as depicted in Table III. Training with a much smaller dataset while attaining a significantly higher mean DSC supports our hypothesis. Compared to the vanilla 3D U-Net, all other methods outperformed it in terms of DSC and Jaccard, although they demonstrated smaller DSC and HD95 scores for both artery and vein. Our method achieved a DSC of 77.26%, a Jaccard of 64.13%, a NSD of 0.86, and an HD95 of 13.72 for arteries, outperforming the baseline universal model [24] by 7.02% in DSC and 5.93% in Jaccard, as well as surpassing the supervised self-configuring model nnU-Net by 9.74% in DSC and 7.68% in Jaccard. Additionally, it outperformed the attention-based self-configuring model nnFormer by 12.8% in DSC and 12.81% in Jaccard. Overall, our model significantly surpasses all other compared methods, achieving superior state-of-the-art performance. Furthermore, Figure 3 displays the visualization of segmentation results for our method and others, illustrating that our method segments both veins and arteries closer to the ground truth.

VI. CONCLUSION

This work introduces a novel segmentation framework, integrating language-vision models with a self-adaptive feature learning pipeline and a designated data augmentation strategy. We leverage our partially annotated dataset to adhere to the best practices from large vision-language models. The framework incorporates our proposed adapter for fine-tuning CLIP embeddings, enhanced with self-attention to capture inter-class relationships. Furthermore, a cross-attention mechanism is seamlessly integrated to promote the effective fusion of the vision model with the segmentation model. We present the most extensive clinical dataset to date for pulmonary artery vein segmentation, comprising 718 high-quality CT volumes.

Empirical evaluation demonstrates that our framework sets a new benchmark on this dataset, achieving an average DSC of 76.22% on a test set of 143 volumes, surpassing nnU-Net by over 10%. These results affirm the superiority of our framework in the challenging task of pulmonary vessel segmentation against current state-of-the-art methods.

REFERENCES

- [1] Chengyan Yuan, Shuni Song, Jinzhong Yang, Yu Sun, Benqiang Yang, and Lisheng Xu, "Pulmonary arteries segmentation from ct images using pa-net with attention module and contour loss," *Medical Physics*, vol. 50, no. 8, pp. 4887–4898, 2023.
- [2] Yanda Meng, Hongrun Zhang, Yitian Zhao, Dongxu Gao, Barbra Hamill, Godhuli Patri, Tunde Peto, Savita Madhusudhan, and Yalin Zheng, "Dual consistency enabled weakly and semi-supervised optic disc and cup segmentation with dual adaptive graph convolutional networks," *IEEE transactions on medical imaging*, vol. 42, no. 2, pp. 416–429, 2022.
- [3] Yanda Meng, Yuchen Zhang, Jianyang Xie, Jinming Duan, Yitian Zhao, and Yalin Zheng, "Weakly/semi-supervised left ventricle segmentation in 2d echocardiography with uncertain region-aware contrastive learning," in *Chinese Conference on Pattern Recognition and Computer Vision (PRCV)*. Springer, 2023, pp. 98–109.
- [4] Yanda Meng, Yuchen Zhang, Jianyang Xie, Jinming Duan, Martha Joddrell, Savita Madhusudhan, Tunde Peto, Yitian Zhao, and Yalin Zheng, "Multi-granularity learning of explicit geometric constraint and contrast for label-efficient medical image segmentation and differentiable clinical function assessment," *Medical Image Analysis*, vol. 95, pp. 103183, 2024.
- [5] Yanda Meng, Xu Chen, Hongrun Zhang, Yitian Zhao, Dongxu Gao, Barbra Hamill, Godhuli Patri, Tunde Peto, Savita Madhusudhan, and Yalin Zheng, "Shape-aware weakly/semi-supervised optic disc and cup segmentation with regional/marginal consistency," in *International Conference on Medical Image Computing and Computer-Assisted Intervention*. Springer, 2022, pp. 524–534.
- [6] Hui Meng, Haochen Zhao, Deqian Yang, Songping Wang, and Zhenpeng Li, "Coarse to fine segmentation method enables accurate and efficient segmentation of organs and tumor in abdominal ct," in *MICCAI Challenge on Fast and Low-Resource Semi-supervised Abdominal Organ Segmentation*, pp. 115–129. Springer, 2023.
- [7] Hui Meng, Haochen Zhao, Ziniu Yu, Qingfeng Li, and Jianwei Niu, "Uncertainty-aware mean teacher framework with inception and squeeze-and-excitation block for miccai flare22 challenge," in *MICCAI Challenge on Fast and Low-Resource Semi-supervised Abdominal Organ Segmentation*, pp. 245–259. Springer, 2022.
- [8] Haochen Zhao, Jianwei Niu, Hui Meng, Yong Wang, Qingfeng Li, and Ziniu Yu, "Focal u-net: A focal self-attention based u-net for breast lesion segmentation in ultrasound images," in *2022 44th Annual International Conference of the IEEE Engineering in Medicine & Biology Society (EMBC)*. IEEE, 2022, pp. 1506–1511.
- [9] Haochen Zhao, Hui Meng, Deqian Yang, Xiaozhe Wu, Qingfeng Li, Jianwei Niu, et al., "Guidednet: Semi-supervised multi-organ segmentation via labeled data guide unlabeled data," in *ACM Multimedia 2024*.

- [10] Deqian Yang, Haochen Zhao, Gaojie Jin, Hui Meng, and Lijun Zhang, "Class-aware cross pseudo supervision framework for semi-supervised multi-organ segmentation in abdominal ct scans," in *Pattern Recognition and Computer Vision*, Zhouchen Lin, Ming-Ming Cheng, Ran He, Kurban Ubul, Wushouer Silamu, Hongbin Zha, Jie Zhou, and Cheng-Lin Liu, Eds., Singapore, 2025, pp. 148–162, Springer Nature Singapore.
- [11] Alec Radford, Jong Wook Kim, Chris Hallacy, Aditya Ramesh, Gabriel Goh, Sandhini Agarwal, Girish Sastry, Amanda Askell, Pamela Mishkin, Jack Clark, et al., "Learning transferable visual models from natural language supervision," in *International conference on machine learning*, PMLR, 2021, pp. 8748–8763.
- [12] Kaiming He, Haoqi Fan, Yuxin Wu, Saining Xie, and Ross Girshick, "Momentum contrast for unsupervised visual representation learning," in *Proceedings of the IEEE/CVF conference on computer vision and pattern recognition*, 2020, pp. 9729–9738.
- [13] Jianwei Yang, Chunyuan Li, Pengchuan Zhang, Bin Xiao, Ce Liu, Lu Yuan, and Jianfeng Gao, "Unified contrastive learning in image-text-label space," in *Proceedings of the IEEE/CVF Conference on Computer Vision and Pattern Recognition*, 2022, pp. 19163–19173.
- [14] Pengfei Liu, Weizhe Yuan, Jinlan Fu, Zhengbao Jiang, Hiroaki Hayashi, and Graham Neubig, "Pre-train, prompt, and predict: A systematic survey of prompting methods in natural language processing," *ACM Computing Surveys*, vol. 55, no. 9, pp. 1–35, 2023.
- [15] Peng Gao, Shijie Geng, Renrui Zhang, Teli Ma, Rongyao Fang, Yongfeng Zhang, Hongsheng Li, and Yu Qiao, "Clip-adapter: Better vision-language models with feature adapters," *International Journal of Computer Vision*, vol. 132, no. 2, pp. 581–595, 2024.
- [16] Alexander Kirillov, Eric Mintun, Nikhila Ravi, Hanzi Mao, Chloe Rolland, Laura Gustafson, Tete Xiao, Spencer Whitehead, Alexander C Berg, Wan-Yen Lo, et al., "Segment anything," in *Proceedings of the IEEE/CVF International Conference on Computer Vision*, 2023, pp. 4015–4026.
- [17] Haoyu Wang, Sizheng Guo, Jin Ye, Zhongying Deng, Junlong Cheng, Tianbin Li, Jianpin Chen, Yanzhou Su, Ziyang Huang, Yiqing Shen, Bin Fu, Shaoting Zhang, Junjun He, and Yu Qiao, "Sam-med3d," 2023.
- [18] Jun Ma, Yuting He, Feifei Li, Lin Han, Chenyu You, and Bo Wang, "Segment anything in medical images," *Nature Communications*, vol. 15, no. 1, pp. 654, 2024.
- [19] Fabian Isensee, Paul F Jaeger, Simon AA Kohl, Jens Petersen, and Klaus H Maier-Hein, "nnu-net: a self-configuring method for deep learning-based biomedical image segmentation," *Nature methods*, vol. 18, no. 2, pp. 203–211, 2021.
- [20] Hong-Yu Zhou, Jiansen Guo, Yinghao Zhang, Lequan Yu, Liansheng Wang, and Yizhou Yu, "nnformer: Interleaved transformer for volumetric segmentation," *arXiv preprint arXiv:2109.03201*, 2021.
- [21] Chao Jia, Yinfei Yang, Ye Xia, Yi-Ting Chen, Zarana Parekh, Hieu Pham, Quoc Le, Yun-Hsuan Sung, Zhen Li, and Tom Duerig, "Scaling up visual and vision-language representation learning with noisy text supervision," in *International conference on machine learning*. PMLR, 2021, pp. 4904–4916.
- [22] Weixiong Lin, Ziheng Zhao, Xiaoman Zhang, Chaoyi Wu, Ya Zhang, Yanfeng Wang, and Weidi Xie, "Pmc-clip: Contrastive language-image pre-training using biomedical documents," in *International Conference on Medical Image Computing and Computer-Assisted Intervention*. Springer, 2023, pp. 525–536.
- [23] Sheng Zhang, Yanbo Xu, Naoto Usuyama, Hanwen Xu, Jaspreet Bagga, Robert Tinn, Sam Preston, Rajesh Rao, Mu Wei, Naveen Valluri, et al., "Biomedclip: a multimodal biomedical foundation model pre-trained from fifteen million scientific image-text pairs," *arXiv preprint arXiv:2303.00915*, 2023.
- [24] Jie Liu, Yixiao Zhang, Jie-Neng Chen, Junfei Xiao, Yongyi Lu, Bennett A Landman, Yixuan Yuan, Alan Yuille, Yucheng Tang, and Zongwei Zhou, "Clip-driven universal model for organ segmentation and tumor detection," in *Proceedings of the IEEE/CVF International Conference on Computer Vision*, 2023, pp. 21152–21164.
- [25] Yixiao Zhang, Xinyi Li, Huimiao Chen, Alan L Yuille, Yaoyao Liu, and Zongwei Zhou, "Continual learning for abdominal multi-organ and tumor segmentation," in *International conference on medical image computing and computer-assisted intervention*. Springer, 2023, pp. 35–45.
- [26] Michela Antonelli, Annika Reinke, Spyridon Bakas, Keyvan Farahani, Annette Kopp-Schneider, Bennett A Landman, Geert Litjens, Bjoern Menze, Olaf Ronneberger, Ronald M Summers, et al., "The medical segmentation decathlon," *Nature communications*, vol. 13, no. 1, pp. 4128, 2022.
- [27] Yulei Qin, Hao Zheng, Yun Gu, Xiaolin Huang, Jie Yang, Lihui Wang, Feng Yao, Yue-Min Zhu, and Guang-Zhong Yang, "Learning tubule-sensitive cnns for pulmonary airway and artery-vein segmentation in ct," *IEEE transactions on medical imaging*, vol. 40, no. 6, pp. 1603–1617, 2021.
- [28] Lufei Lou, Yu Xin, Jiangbo Qian, and Yihong Dong, "A detail-oriented reper-2d network for pulmonary artery segmentation," *Biomedical Signal Processing and Control*, vol. 93, pp. 106183, 2024.
- [29] Gongning Luo, Kuanquan Wang, Jun Liu, Shuo Li, Xinjie Liang, Xiangyu Li, Shaowei Gan, Wei Wang, Suyu Dong, Wenyi Wang, et al., "Efficient automatic segmentation for multi-level pulmonary arteries: The parse challenge," *arXiv preprint arXiv:2304.03708*, 2023.
- [30] Foivos I Diakogiannis, François Waldner, Peter Caccetta, and Chen Wu, "Resunet-a: A deep learning framework for semantic segmentation of remotely sensed data," *ISPRS Journal of Photogrammetry and Remote Sensing*, vol. 162, pp. 94–114, 2020.
- [31] Hao Qi, Ming Wu, Sunkui Ke, Xiangxing Chen, Hui-Qing Zeng, Yinran Chen, and Xiongbiao Luo, "Deep residual w-unit learning with semantic embedding for automatic pulmonary ct artery-vein separation," in *ICASSP 2024-2024 IEEE International Conference on Acoustics, Speech and Signal Processing (ICASSP)*. IEEE, 2024, pp. 3275–3279.
- [32] Arnaud Arindra Adiyoso Setio, Alberto Traverso, Thomas De Bel, Moira SN Berens, Cas Van Den Bogaard, Piergiorgio Cerello, Hao Chen, Qi Dou, Maria Evelina Fantacci, Bram Geurts, et al., "Validation, comparison, and combination of algorithms for automatic detection of pulmonary nodules in computed tomography images: the luna16 challenge," *Medical image analysis*, vol. 42, pp. 1–13, 2017.
- [33] Xiao Liu, Fanjin Zhang, Zhenyu Hou, Li Mian, Zhaoyu Wang, Jing Zhang, and Jie Tang, "Self-supervised learning: Generative or contrastive," *IEEE transactions on knowledge and data engineering*, vol. 35, no. 1, pp. 857–876, 2021.
- [34] Kaiming He, Xiangyu Zhang, Shaoqing Ren, and Jian Sun, "Deep residual learning for image recognition," in *Proceedings of the IEEE conference on computer vision and pattern recognition*, 2016, pp. 770–778.
- [35] Alexey Dosovitskiy, Lucas Beyer, Alexander Kolesnikov, Dirk Weissenborn, Xiaohua Zhai, Thomas Unterthiner, Mostafa Dehghani, Matthias Minderer, Georg Heigold, Sylvain Gelly, et al., "An image is worth 16x16 words: Transformers for image recognition at scale," *arXiv preprint arXiv:2010.11929*, 2020.
- [36] Jacob Devlin, "Bert: Pre-training of deep bidirectional transformers for language understanding," *arXiv preprint arXiv:1810.04805*, 2018.
- [37] Yuqi Lin, Minghao Chen, Wenxiao Wang, Boxi Wu, Ke Li, Binbin Lin, Haifeng Liu, and Xiaofei He, "Clip is also an efficient segmenter: A text-driven approach for weakly supervised semantic segmentation," in *Proceedings of the IEEE/CVF Conference on Computer Vision and Pattern Recognition*, 2023, pp. 15305–15314.
- [38] Ziqin Zhou, Yinjie Lei, Bowen Zhang, Lingqiao Liu, and Yifan Liu, "Zegclip: Towards adapting clip for zero-shot semantic segmentation," in *Proceedings of the IEEE/CVF Conference on Computer Vision and Pattern Recognition*, 2023, pp. 11175–11185.
- [39] Ilya Loshchilov and Frank Hutter, "Decoupled weight decay regularization," *arXiv preprint arXiv:1711.05101*, 2017.
- [40] Olaf Ronneberger, Philipp Fischer, and Thomas Brox, "U-net: Convolutional networks for biomedical image segmentation," in *Medical image computing and computer-assisted intervention—MICCAI 2015: 18th international conference, Munich, Germany, October 5-9, 2015, proceedings, part III 18*. Springer, 2015, pp. 234–241.